

Evaluation of Passive Carrier-Suppression Techniques for UHF RFID Systems

Lukas W. Mayer, Robert Langwieser, and Arpad L. Scholtz

Institute of Communications and Radio-Frequency Engineering Vienna University of Technology
Gusshausstrae 25, 1040 Vienna, Austria, lukas.mayer@nt.tuwien.ac.at

Abstract—In this paper we investigate the signal that is returned from an interrogator antenna when communicating with a radio-frequency identification (RFID) transponder at a carrier frequency of 866 MHz. This signal contains the response of the transponder and also a part of the carrier signal that is leaking into the receive path. Depending on the type of interrogator antenna configuration used, both signal components are expected to vary widely in terms of power.

We perform measurements with patch antennas that radiate linearly and circularly polarized waves in various configurations. Furthermore, passive methods that minimize the leaking carrier are explored and compared. Results are obtained for transponder positions covering the transition region between near- and far-field. It is found that separated transmitter and receiver antennas offer highest carrier-suppression and thus require the least effort for the receiver.

Index Terms—UHF propagation, antenna proximity factors.

I. INTRODUCTION

A critical issue in the design of a radio-frequency identification (RFID) interrogator frontend is the suppression of the carrier signal that is unintentionally leaking into the receive path. The interrogator has to transmit a strong carrier signal to supply passive transponders with sufficient operating power. The response of the transponder on the other hand is generated by passive backscattering, which is achieved by a modulation of the transponder chip's input impedance. Since only a small fraction of the power incident upon the transponder is reradiated, the signal received by the interrogator's antenna is very weak compared to the transmitted carrier signal.

Several methods can be used to separate the transmitted from the received signal. Although very high performance can be expected from advanced techniques like active carrier cancellers [1] or specialized active antennas [2], descent carrier-suppression can be achieved with a circulator, directional coupler, or—even simpler—separate antennas for transmitting and receiving. In many cases, passive techniques are sufficient whereas in advanced interrogator frontend designs they are usually succeeded by active carrier cancellers and carrier-suppression algorithms that are performed in digital baseband hardware.

This contribution focuses on passive carrier-suppression techniques. The antennas and antenna configurations investigated are described in Sec. II. The measurement setup that is used to analyze each setup is described in Sec. III.

This work has been funded by the Christian Doppler Laboratory for Wireless Technologies for Sustainable Mobility. Furthermore, our industrial partner Infineon Technologies has to be thanked for enabling this work.

Measurement results are discussed in Sec. IV and conclusions are drawn in Sec. V.

II. PASSIVE CARRIER-SUPPRESSION TECHNIQUES

In this section we describe the interrogator antennas and the carrier-suppression techniques that we analyzed in our experiments. A rather theoretical analysis of similar setups is given in [3]. For a fair comparison of different antenna setups, we constructed microstrip patch antennas that radiate linearly polarized waves. Each antenna has two feeds, one exciting the horizontal and one the vertical mode of the patch. From simulations with Ansoft HFSS the efficiency of these antennas was estimated to be better than 95%. The antenna's peak gain is 9.5 dBi. For radiating and receiving linearly polarized waves, each feed was joined with the inner conductor of a coaxial flange connector mounted directly at the back of the ground plane. A cross-polar discrimination of more than 30 dB is achieved.

For transmitting left-hand circularly polarized (LHCP) or a right-hand circularly polarized (RHCP) waves, the patch antennas that originally radiate horizontal and vertical polarization were connected with a 3 dB branch line coupler. This circuit splits the signal fed into its transmit input into equal parts with a 90° phase offset. When fed into the antenna, these signals cause LHCP radiation. On the other hand the coupler combines the antenna signals caused by an incident RHCP wave at its output port. The coupler introduces losses of less than one decibel. The cross-polar discrimination of these circularly polarized antennas is better than 25 dB.

Throughout this work, passive carrier-suppression methods are evaluated. The antenna configurations that we have analyzed are depicted in Fig. 1 and explained in the following:

- A linearly polarized patch antenna equipped with a circulator that separates the transmitted from the received wave. The imperfect matching of the antenna and the finite isolation of the circulator cause a leakage of the carrier signal into the receive path. In a second experiment, an impedance-tuner was inserted between the circulator and the antenna. With this tuner, perfect matching between the circulator and the antenna can be achieved, which—in theory—allows to fully cancel the effects of the imperfect elements.
- A circularly polarized patch antenna equipped with a circulator. Again, in a further experiment, an impedance-tuner was inserted between the antenna and the circulator to establish optimal matching.

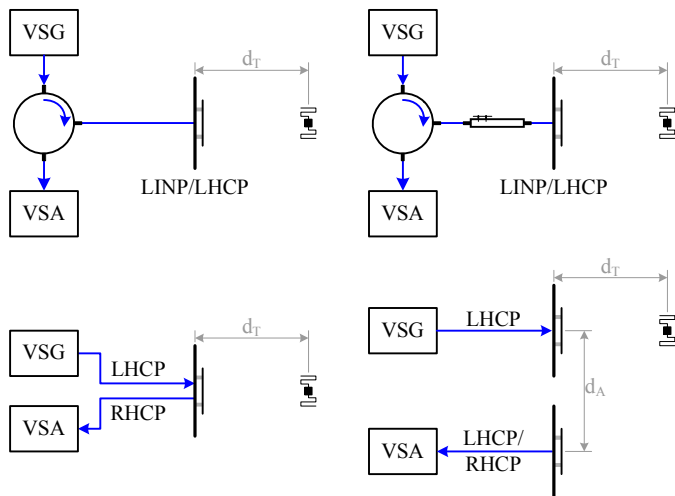


Fig. 1. Measurement setups. Top: One-port antenna systems with a circulator or with a circulator and an impedance-tuner to separate transmitted and received signals. Bottom: Two-port setups with a dual-polarized antenna or with separate transmit and receive antennas.

- A patch antenna simultaneously radiating an LHCP wave and receiving an RHCP wave.
- Two separate circularly polarized antennas, one for transmitting and one for receiving. The antennas are aligned next to each other with a spacing of $d_A = 400$ mm or $d_A = 670$ mm (measured between the patch centers). Both, a left-hand and a right-hand circularly polarized antenna were used for receiving whereas an LHCP wave was radiated by the transmit antenna.

III. MEASUREMENT SETUP

With the procedure described in this section, a fair comparison of the above mentioned antenna configurations is possible. To obtain most general results the measurement campaign was performed in an empty chamber where some microwave absorbers were placed to reduce, but not to fully avoid multipath propagation.

An R&S SMU200A vector signal generator (VSG) serves as a transmit signal source. The transmit signal was modulated with an EPCGlobal Gen2 standard compliant wake-up sequence that contains a query command and requires the transponder to respond with a preamble and a 16 bit random number encoded in the FM0 modulation scheme at a link frequency of 148 kHz. To record the receive signal of each antenna configuration, an R&S FSQ26 vector signal analyzer (VSA) was used. It provides baseband IQ-samples of the receive signal which were then analyzed in Matlab. First, the power of the continuous carrier signal P_{Leak} was calculated. P_{Leak} results from the superposition of the following signal components:

- Leakage of the respective antenna configuration.
- Received signals that result from multipath propagation in the chamber.
- The receive signal that is generated by reflection in the structural mode [4] of the transponder antenna. It

is caused by the transponder antenna metal and is not influenced by the matching situation at the transponder antenna port.

- The purely sinusoidal part of the signal reflected at the transponder chip input $Y_{CW}(t)$ that is reradiated by the tag antenna and received by the interrogator antenna.

The last item needs some more explanation: For responding the transponder chip switches between two impedance states. For each of these impedance states magnitude and phase of the signal reflected at the transponder chip's input is a function of the antenna impedance and the respective chip impedance. The reflected signal $Y(t)$ can thus be considered as vector modulated. Such a signal can be decomposed into two parts: The first part is a continuous wave signal $Y_{CW}(t)$ —the one that is mentioned above—and the second part is a purely phase modulated signal $Y_{PM}(t)$ which has constant envelope—the response signal. With this decomposition the resulting phase difference between the states of the response signal $Y_{PM}(t)$ is always 180° . Where $Y_{CW}(t)$ contains no information and can not be distinguished from static reflections in space, $Y_{PM}(t)$ contains the information of the impedance switching done by the transponder chip. In the frequency domain, the response signal appears as sidebands located to the left and right of the carrier.

From the received $Y_{PM}(t)$ the response of the transponder is detected and the complex amplitudes of the two states are estimated. Consequently, the power of the received response signal P_{PM} is calculated. With the total carrier power P_{Leak} , the signal-to-carrier ratio $\beta = P_{PM}/P_{Leak}$ is determined.

For testing a UPM Dogbone transponder was selected because it features an efficient linearly polarized dipole antenna. The transponder was mounted on a motor-driven cord that extends from the transmit antenna. The transponder position was varied in 25 mm ($0.06 \lambda_0$) steps within a range d_T of 6 cm to 3 m. For each antenna setup a distance sweep was done at a peak-envelope transmit power of $P_{Tx} = 20$ dBm and a carrier frequency of 866 MHz.

IV. MEASUREMENT RESULTS

First, the antenna configurations were analyzed for their ability to separate the transmit signal from the received signal. The Tx/Rx-separation α which is defined by the ratio of the transmitted and the received power at the interrogator frontend is defined by $\alpha = P_{Tx}/P_{Rx}$. In principle this Tx/Rx-separation α is a property of the antenna configuration when operated in free space. In our experiments we measure α in a low fading environment. Furthermore, we determine the influence of one single RFID transponder, that is positioned in front of the transmit antenna.

Fig. 2 shows the Tx/Rx-separation α as a function of the distance d_T between the transponder and the interrogator antenna. The four graphs are measurement results for antenna configurations that feature only one antenna port for both transmitting and receiving. The lower two graphs represent two setups where a circulator (RADITEK, RC-860-900-ee1-N23-10WR-sj with measured isolation of 34 dB) is directly

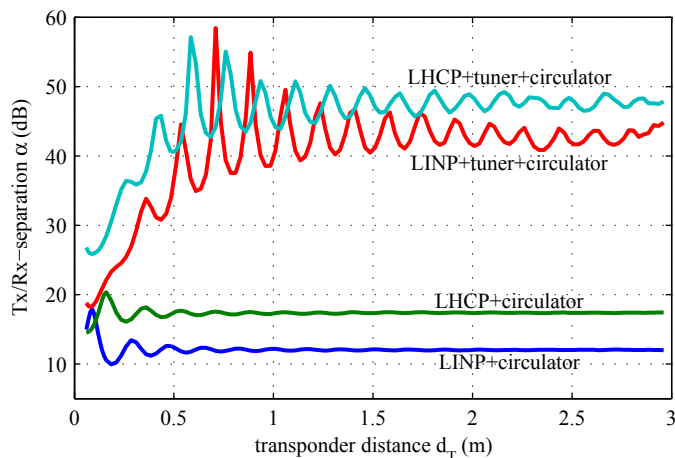


Fig. 2. Tx/Rx-separation versus distance d_T for one-port setups.

connected to the interrogator antenna for separating the transmitted from the received signal. When operated in free space, the return loss of the antenna limits the Tx/Rx-separation. In general, a return loss of some 10 dB to 20 dB is typical for commercially available antennas. With a high-quality circulator, this return loss can be well preserved and converted into Tx/Rx-separation. In real-world RFID scenarios however, transponders and objects might be present in the near field of the interrogator antenna. This causes a detuning of the antenna which degrades the antenna's return loss. Consequently, the carrier signal returned by the antenna R_{Mismatch} increases.

If the antenna receives waves that result from reflections in space, the Tx/Rx-separation is influenced as well. A transponder that is positioned in front of the antenna, for instance, will reflect some power in its structural antenna mode. This reflected wave is received and causes a signal R_{Tag} at the interrogator antenna port. Depending on the position of the transponder R_{Tag} varies in amplitude and phase. At the receiver the superposition $R = R_{\text{Tag}} + R_{\text{Mismatch}}$ of the two signals is observed.

Especially at low transponder distance d_T the reflected signal R_{Tag} is strong and causes a variation of the Tx/Rx-separation α . This is particularly pronounced with a linearly polarized antenna. With the circularly polarized antenna the variation of α is weaker. The reason of this is that the reflected signal R_{Tag} is lowered by 6 dB because of the polarization mismatch with the linearly polarized transponder antenna (3 dB are lost in each, forward- and return-link).

The upper graphs in Fig. 2 show the Tx/Rx-separation if the antennas are optimally matched with the circulator. This is achieved by inserting and adjusting an impedance-tuner that increases the return loss of the interrogator antenna and consequently reduces R_{Mismatch} . The received signal R_{Tag} on the other hand will be marginally increased by the improvement in matching. Indeed, if the transponder is far away from the interrogator antenna and its reflected signal R_{Tag} is weak, the Tx/Rx-separation improves by more than 25 dB. If the transponder is brought closer to the interrogator antenna, R_{Tag} increases and causes a strong variation in α . If the transponder

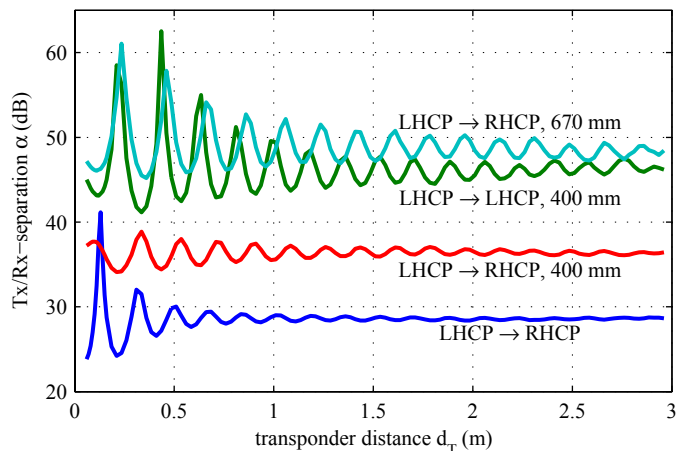


Fig. 3. Tx/Rx-separation versus distance d_T for two-port setups.

is very close ($d_T < 0.3$ m), the interrogator antenna is detuned and R_{Mismatch} prevails. This leads to a decrease of the Tx/Rx-separation by about 15 dB.

In Fig. 3 the Tx/Rx-separation of the two-port setups is shown versus distance d_T . For the dual circularly polarized antenna (LHCP→RHCP), Tx/Rx-separation is approximately equivalent to the cross-polar discrimination of the antenna. In free space this interrogator antenna provides an α of 28 dB. This is quite an improvement compared to single port antennas that use a circulator, and is achieved at relatively low cost. Like in the one-port configurations the signal reflected by the transponder contributes to the receive signal. If the transponder is close to the interrogator antenna, a stronger variation of α is observed.

If separate interrogator antennas are used for transmitting and receiving (bi-static arrangement), the quality and tuning of the antennas are less important. With two antennas of orthogonal circular polarization, a Tx/Rx-separation of $\alpha = 36$ dB was achieved at an antenna spacing of $d_A = 400$ mm (LHCP→RHCP, 400 mm). Since the antennas are within the Rayleigh distance of each other, direct coupling between the patches likely causes the leakage. When a transponder is positioned in front of the transmitting antenna, its reflected wave is picked up by the receiving antenna. This again causes a variation of α . Depending on the angle of arrival, the reflected wave is weighed by the directional pattern of the receiving antenna. Consequently, if the transponder is brought very close to the transmitting antenna, the reflected signal R_{Tag} is weaker. In the measurement result this can be seen as a slight decrease in the variation of α at distances smaller than 0.25 m.

If a left-hand circularly polarized antenna is used for receiving as well, α is increased by another 12 dB as long as no transponder is present (LHCP→LHCP, 400 mm). We suppose that this is caused by a reduction of the direct coupling between antennas of same polarization. Since the coupled signal is weaker in this setup, the signal reflected at the transponder causes a stronger variation in the Tx/Rx-separation. When increasing the antenna spacing to $d_A = 670$ mm, α increases further, even if orthogonal polarizations

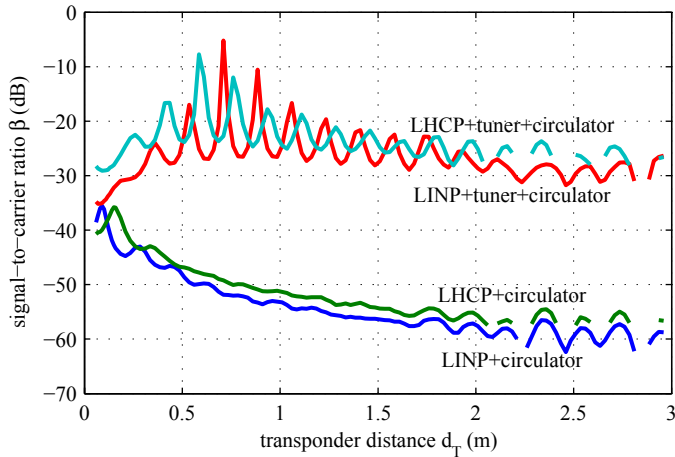


Fig. 4. Signal-to-carrier ratio versus distance d_T for one-port setups.

are employed (LHCP→RHCP, 670 mm). Again, a slight decrease of the variation in α is observed when the transponder is brought very close to the transmitting antenna.

In Fig. 4 and Fig. 5, the signal-to-carrier ratio β of the received signal is shown for the one-port and the two-port setups, respectively. Unlike the Tx/Rx-separation, that relates the power of the transmitted signal with the power of the received signal, the signal-to-carrier ratio analyzes only the received signal in terms of the sinusoidal carrier power P_{Leak} and the power of the actual response signal P_{PM} produced by backscatter modulation at the transponder chip. The signal-to-carrier ratio is thus a measure for the necessary dynamic range of the receiver. When digital signal processing hardware is used to analyze the response of the transponder, β is related to the number of bits that are necessary for digitalization.

For a transponder distance of $d_T > 1.5$ m, fading sets in which—at some spots—disables the communication with the transponder. There, no β value can be calculated and consequently the graphs show gaps. From the graphs at the bottom of Fig. 4 it can be seen that communication is more reliable with a linearly polarized transmit antenna. This is because in our measurement the interrogator and the transponder antenna are both aligned to radiate in vertical polarization. On the other hand, with the circularly polarized interrogator antenna, 3 dB are lost in the forward-link but robustness to transponder orientation is improved.

From all graphs in Fig. 4 and 5 it is seen that the signal-to-carrier ratio β is strongly influenced by the Tx/Rx-separation α . Antenna setups that provide decent α also show higher β . For one-port antenna setups with a circulator, a signal-to-carrier ratio of $\beta = -64$ dB was measured for the linearly polarized antenna and the Dogbone transponder at read ranges of approximately 2.5 m. This shows that when using a circulator only, the return-loss of the interrogator antenna has a strong impact on the dynamic range required for detecting the response signal. With a very well matched antenna (achieved with an impedance-tuner), β improves significantly by about 30 dB. However, as soon as transponders or objects are brought close to the interrogator antenna β again drops.

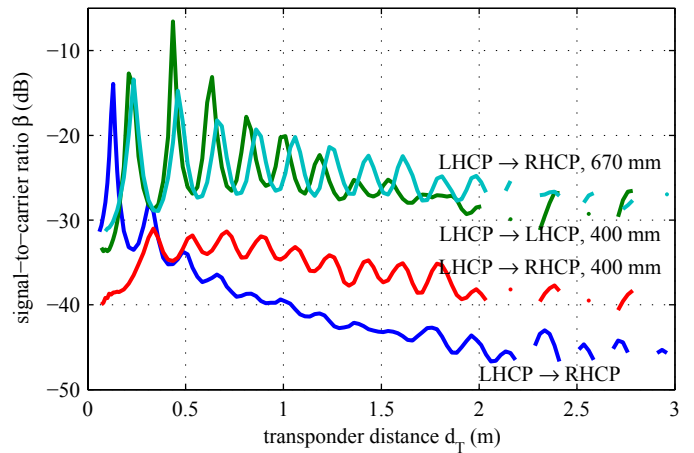


Fig. 5. Signal-to-carrier ratio versus distance d_T for two-port setups.

With setups that have separate transmit and receive antennas a drop in β is observed at low transponder distance d_T also. This can be seen in Fig. 5. But here, the drop is rather caused by the transponder being located in the low-gain region of the receive antenna which consequently reduces the received power P_{PM} .

V. CONCLUSION

The measurement results show that the Tx/Rx-separation α and the signal-to-carrier ratio β of one-port antenna setups that feature a high quality circulator can only compete with two-port setups if the antennas are very well matched—a condition which is hardly satisfied in realistic RFID scenarios.

More solid performance at relatively low cost can be achieved with a patch antenna that simultaneously radiates a left-hand and receives a right-hand circularly polarized wave. Here an α of more than 25 dB was achieved. Also, β was improved by 10 dB compared to the conventional one-port setups we investigated.

If the application allows to use separate antennas, α and β can be improved further. The coplanar arrangement of circularly polarized patch antennas outperform all other setups. However, a slight drop in performance was observed when the transponder was located close to the transmit antenna thus being in the low-gain region of the receive antenna. It is also interesting to note, that when separate antennas are used, patch antennas of same circular polarization show better performance than patch antennas of opposite polarization.

REFERENCES

- [1] G. Lasser, R. Langwieser, and A. L. Scholtz, "Broadband suppression properties of active leaking carrier cancellers," in *Proc. IEEE International Conference on RFID*, Apr. 2009.
- [2] L. W. Mayer and A. L. Scholtz, "Circularly polarized patch antenna with high Tx/Rx-separation," in *Proc. IEEE International Conference on RFID*, Apr. 2009.
- [3] K. Penttilä, L. Sydänheimo, and M. Kivikoski, "Implementation of Tx/Rx isolation in an RFID reader," *Int. J. Radio Frequency Identification Technology and Applications*, vol. 1, no. 1, pp. 74–89, 2006.
- [4] R. C. Hansen, "Relationships between antennas as scatterers and as radiators," *Proceedings of the IEEE*, vol. 77, no. 5, pp. 659–662, May 1989.